

Electroweak corrections to Z + 2 jets production at the LHC

Ansgar Denner*

Universität Würzburg

E-mail: denner@physik.uni-wuerzburg.de

Lars Hofer†

Universität Würzburg

E-mail: lhofer@ifae.es

Andreas Scharf

Universität Würzburg

E-mail: ascharf@physik.uni-wuerzburg.de

Sandro Uccirati

Università di Torino

E-mail: uccirati@to.infn.it

We present results for the electroweak radiative corrections to the production of a leptonically decaying Z boson in association with two jets at the LHC. Tree-level and one-loop amplitudes have been obtained with the computer code RECOLA for the recursive generation of tree-level and one-loop amplitudes in the Standard Model. The one-loop integrals have been calculated with the tensor-integral library COLLIER. The electroweak corrections turn out to be small for inclusive cross sections but can become large in tails of distributions.

11th International Symposium on Radiative Corrections (Applications of Quantum Field Theory to Phenomenology)

22-27 September 2013

Lumley Castle Hotel, Durham, UK

*Speaker.

†Present address: Universitat Autònoma de Barcelona.

1. Introduction

The discovery of a Higgs boson with a mass of around 125 GeV was a spectacular success of the Standard Model (SM). Having completed the particle spectrum of the SM, the task is to scrutinise this model in all details and to search for experimental signals showing deviations from their SM predictions. This includes the detailed investigation of the observed Higgs boson as well as precise measurements of all kind of SM processes. For an adequate comparison between theory and experiment higher-order perturbative corrections are indispensable. This concerns in the first place QCD corrections, which are typically of the order of several ten per cent or more, and even next-to-next-to-leading order (NNLO) QCD corrections are needed for several processes. However, also electroweak (EW) corrections are mandatory for many processes at the LHC. While they are often (but not always) small for inclusive observables, they can be enhanced by kinematic effects, in particular near resonances, or where high-energy scales matter, like in tails of distributions. They can easily reach several ten per cent for energy scales in the TeV region.

In the past years, huge progress has been made in the automation of the calculation of next-to-leading order (NLO) QCD corrections. Different groups have developed software packages [1, 2, 3, 4, 5, 6, 7, 8] and used them to perform complicated calculations. The efforts have concentrated mostly on QCD corrections (examples can be found in these proceedings). Recently we have constructed RECOLA, a generator of one-loop (and tree) amplitudes in the full SM [9, 10], including EW corrections. It is based on an algorithm which uses recursion relations for the computation of the coefficients of the tensor integrals [11].

As a first application of RECOLA we have chosen the process $pp \rightarrow Z + 2\text{jets} \rightarrow l^+l^- + 2\text{jets}$. Owing to its large cross section and similar signatures it provides a major background for Higgs-boson production in vector-boson fusion kinematics and allows to study the systematics for the $H + 2\text{jets}$ final state. The dominant NLO QCD corrections of $\mathcal{O}(\alpha_s^3\alpha^2)$ have been investigated in Refs. [12], while a subset of EW $Z + 2\text{jets}$ production has been studied at NLO QCD in Ref. [13]. Electroweak Sudakov corrections have been considered in Ref. [14]. Our aim is the calculation of the complete EW corrections of $\mathcal{O}(\alpha_s^2\alpha^3)$.

2. COLLIER, a Fortran library for tensor one-loop integrals

A general one-loop amplitude $\delta\mathcal{M}$ can be written as

$$\delta\mathcal{M} = \sum_j \sum_{R_j} c_{\mu_1 \dots \mu_{R_j}}^{(j, R_j, N_j)} T_{(j, R_j, N_j)}^{\mu_1 \dots \mu_{R_j}}, \quad (2.1)$$

where j runs over all appearing tensor integrals with rank R_j and degree (number of propagators) N_j .

While RECOLA calculates the coefficients $c_{\mu_1 \dots \mu_{R_j}}^{(j, R_j, N_j)}$, the tensor integrals

$$T_{(j, R_j, N_j)}^{\mu_1 \dots \mu_{R_j}} = \frac{(2\pi\mu)^{4-D}}{i\pi^2} \int d^D q \frac{q^{\mu_1} \dots q^{\mu_{R_j}}}{D_{j,0} \dots D_{j,N_j-1}}, \quad D_{j,a} = (q + p_{j,a})^2 - m_{j,a}^2 \quad (2.2)$$

are provided by COLLIER, the Complex One-Loop Library with Extended Regularisations [15, 16, 17, 18]. This library is also used by OPENLOOPS [19, 20].

COLLIER is a Fortran library for the numerical evaluation of one-loop scalar and tensor integrals appearing in perturbative calculations in relativistic quantum field theory. It provides tensor integrals with arbitrary rank for N -point functions up to currently $N = 6$, either directly as numerical values for the tensor elements $T_{(j,R_j,N_j)}^{\mu_1 \dots \mu_{R_j}}$ or as numerical values for the invariant coefficients $T_{\underbrace{0 \dots 0}_{2n} i_{2n+1} \dots i_{R_j}}^{(j,R_j,N_j)}$ appearing in the covariant decomposition

$$T_{(j,R_j,N_j)}^{\mu_1 \dots \mu_{R_j}} = \sum_{n=0}^{\lfloor \frac{R_j}{2} \rfloor} \sum_{i_{2n+1}, \dots, i_{R_j}=1}^{N-1} \underbrace{\{g \dots g p \dots p\}}_n^{\mu_1 \dots \mu_{R_j}} T_{\underbrace{0 \dots 0}_{2n} i_{2n+1} \dots i_{R_j}}^{(j,R_j,N_j)}. \quad (2.3)$$

The tensor integrals are evaluated as follows: For 1-point and 2-point tensor integrals explicit numerically stable expressions are used [21]. For 3-point and 4-point functions we employ Passarino–Veltman reduction along with the tensor-integral reduction methods of Ref. [16] which are based on expansions in small determinants. Depending on the specific kinematic configuration a suitable method is selected for each tensor integral. In this way a numerically stable calculation is achieved for almost all configurations. Finally 5-point and 6-point tensor integrals are directly reduced to integrals with lower rank and lower degree using the methods summarised in Refs. [15, 16].

COLLIER includes a complete set of scalar integrals for scattering processes. These are evaluated from analytical expressions as given in Ref. [17, 22]. Ultraviolet singularities are regularised dimensionally, soft and collinear singularities can be regularised either dimensionally or with masses. While complex internal masses, required for unstable particles, are fully supported, external momenta and virtualities must be real.

COLLIER has a built-in cache system to avoid the recalculation of identical integrals and two branches that allow for an independent calculation of each integral via two different implementations and direct numerical cross-checks.

3. $Z + 2$ jets production at the LHC

We consider the production of a leptonically decaying Z boson in association with 2 hard jets. We include diagrams including a resonant Z boson as well as all irreducible background diagrams leading to the $l^+ l^- jj$ final state.

3.1 Leading-order contributions

At leading order (LO), the production of a leptonically decaying Z boson at the LHC in association with a pair of hard jets is governed by the partonic subprocesses

$$q_i g \rightarrow q_i g l^+ l^-, \quad (3.1)$$

$$q_i \bar{q}_i \rightarrow q_j \bar{q}_j l^+ l^-, \quad q_i, q_j = u, c, d, s, b, \quad (3.2)$$

and their crossing-related counterparts. All partonic processes can be constructed from the three basic channels $u g \rightarrow u g l^+ l^-$, $u s \rightarrow u s l^+ l^-$, and $u s \rightarrow d c l^+ l^-$. While the mixed quark–gluon (gluonic) channels (3.1) contribute to the cross section exclusively at order $\mathcal{O}(\alpha_s^2 \alpha^2)$, the four-quark

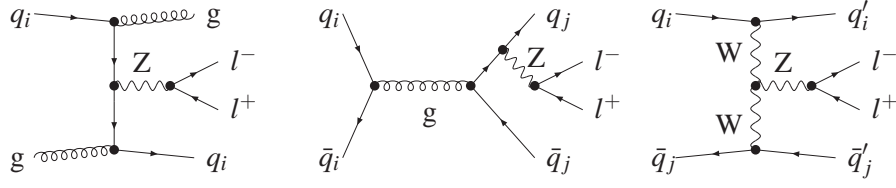


Figure 1: From left to right: Sample tree diagrams for the QCD contributions to $q_i g \rightarrow q_i g l^+ l^-$ and to $q_i \bar{q}_i \rightarrow q_j \bar{q}_j l^+ l^-$, and the EW contributions to $q_i \bar{q}_j \rightarrow q'_i \bar{q}'_j l^+ l^-$.

channels (3.2) involve LO diagrams of strong as well as of EW nature leading to contributions of order $\mathcal{O}(\alpha_s^2 \alpha^2)$, $\mathcal{O}(\alpha_s \alpha^3)$, and $\mathcal{O}(\alpha^4)$. Representative Feynman diagrams are shown in Fig. 1. Photon induced contributions, which are below 0.05%, have been omitted.

3.2 Setup of NLO calculation

Taking into account all one-loop QCD and EW diagrams, the cross section involves contributions of orders $\mathcal{O}(\alpha_s^3 \alpha^2)$, $\mathcal{O}(\alpha_s^2 \alpha^3)$, $\mathcal{O}(\alpha_s \alpha^4)$, and $\mathcal{O}(\alpha^5)$. We are interested in the contributions of $\mathcal{O}(\alpha_s^2 \alpha^3)$ which involve NLO EW corrections to the dominant LO contributions of $\mathcal{O}(\alpha_s^2 \alpha^2)$ and NLO QCD corrections to the LO interference contributions of $\mathcal{O}(\alpha_s \alpha^3)$.

We use the complex-mass scheme [23, 24, 25] to treat resonant Z-boson propagators (see Fig. 2 left for a sample diagram), i.e. we consistently use the complex masses

$$\mu_Z^2 = M_Z^2 - iM_Z \Gamma_Z, \quad \mu_W^2 = M_W^2 - iM_W \Gamma_W \quad (3.3)$$

for the Z and W bosons.

The electromagnetic coupling constant α is defined within the G_μ scheme, i.e. we use

$$\alpha = \frac{\sqrt{2} G_\mu M_W^2}{\pi} \left(1 - \frac{M_W^2}{M_Z^2} \right). \quad (3.4)$$

This definition takes into account higher-order effects of the renormalisation-group running from 0 to M_W^2 . Moreover, the renormalisation of α becomes independent of light quark masses.

3.3 Virtual corrections

The virtual corrections contributing at $\mathcal{O}(\alpha_s^2 \alpha^3)$ involve $\mathcal{O}(1200)$ diagrams for the $u g \rightarrow u g l^+ l^-$ channel, including 18 hexagons and 85 pentagons, and an almost comparable number of diagrams for the $u s \rightarrow u s l^+ l^-$ channel. The most complicated topologies involve 6-point functions up to rank 4 (see Fig. 2 right for a sample diagram). Renormalisation is performed within the complex-mass scheme [24]. As the coupling α_{G_μ} is derived from M_W , M_Z and G_μ , its counterterm inherits a correction term Δr from the weak corrections to muon decay.

In NLO we neglect all channels involving external bottom quarks. At LO these contributions are taken into account and contribute at the per-cent level.

3.4 Real corrections

The real EW corrections of $\mathcal{O}(\alpha_s^2 \alpha^3)$ consist of real photon emission from the LO QCD diagrams in all subprocesses (3.1), i.e. the processes

$$q_i g \rightarrow q_i g l^+ l^- \gamma, \quad (3.5)$$

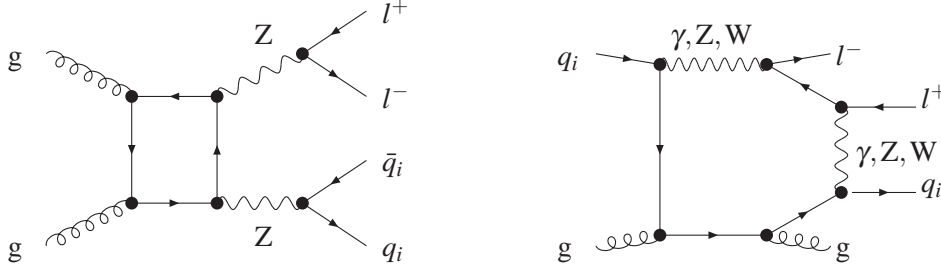


Figure 2: Box diagram involving potentially resonant Z-boson propagators (left) and hexagon diagram involving a 6-point tensor integral of rank 4 (right).

$$q_i \bar{q}_i \rightarrow q_j \bar{q}_j l^+ l^- \gamma, \quad (3.6)$$

and from real gluon emission contributions in the interferences between LO QCD and EW diagrams, i.e. the processes

$$q_i \bar{q}_i \rightarrow q_j \bar{q}_j l^+ l^- g. \quad (3.7)$$

The amplitudes can be constructed in exactly the same way as for the LO, but we only take contributions of $\mathcal{O}(\alpha_s^2 \alpha^3)$ into account.

IR divergences of soft or collinear photons and gluons are regularised dimensionally. We use the Catani–Seymour dipole formalism as formulated in Ref. [26], which we transferred in a straightforward way to the case of dimensionally regularised photon emission.

The presence of gluons in the final state gives rise to a further type of singularity. In IR-safe observables quarks, and thus all QCD partons, have to be recombined with photons if they are sufficiently collinear. Thus, soft gluons can pass the selection cuts if they are recombined with a hard collinear photon, giving rise to a soft-gluon divergence that would be cancelled by the virtual QCD corrections to $Z + 1 \text{ jet} + \gamma$ production. Following Refs. [27] we eliminate this singularity by discarding events containing a jet consisting of a hard photon and a soft parton a ($a = q_i, \bar{q}_i, g$) taking the photon–jet energy fraction $z_\gamma = E_\gamma / (E_\gamma + E_a)$ as a discriminator. Finally, we have to absorb left-over singularities into contributions involving the quark–photon fragmentation function [28].

3.5 Implementation

The calculation was performed using the amplitude generator RECOLA for all tree-level, one-loop and bremsstrahlung amplitudes. This generator is interfaced with the tensor-integral library COLLIER [18]. The phase-space integration is performed by an in-house multi-channel Monte-Carlo generator [29].

The results have been checked by a second independent calculation based on the conventional Feynman-diagrammatic approach. It uses FEYNARTS 3.2 [30, 31], FORMCALC 3.1 [32] and POLE [33] for the generation, simplification and calculation of the Feynman amplitudes. The tensor-integral coefficients are again evaluated by COLLIER, which includes a second independent implementation of all its building blocks. Finally, the phase-space integration is performed with the multi-channel generator LUSIFER [34].

process class	σ^{LO} [fb]	$\sigma^{\text{LO}}/\sigma_{\text{tot}}^{\text{LO}}$ [%]	$\sigma_{\text{EW}}^{\text{NLO}}$ [fb]	$\frac{\sigma_{\text{EW}}^{\text{NLO}}}{\sigma^{\text{LO}}} - 1$ [%]
gluonic	17948(4)	77.3	17534(4)	-2.31
four-quark	5270.0(5)	22.7	5140(2)	-2.46
sum	23218(4)	100	22675(5)	-2.34

Table 1: LO cross section for $pp \rightarrow l^+l^- + 2$ jets at the 8TeV LHC split into contributions from gluonic and four-quark channels. The second column provides the LO cross section with integration error on the last digit in parentheses, the third column contains the relative contribution to the total cross section in per cent, the fourth column the NLO EW cross section, and in the last column the relative EW corrections.

3.6 Numerical results

We present results for the 8TeV LHC with the input parameters as given in Ref. [9]. Since we focus on NLO EW corrections, we stick to the LO MSTW2008LO PDF set [35]. For the QCD factorisation and renormalisation scales we choose $\mu_F = \mu_R = M_Z$. The scale choice as well as the actual value for the strong coupling α_s plays a minor role for our numerical analysis of EW radiative corrections.

The jet clustering is performed with the anti- k_T algorithm [36] with separation parameter $R = 0.4$. We require two hard jets and two charged leptons fulfilling the following requirements

$$\begin{aligned}
 p_{T,\text{jet}} > 30\text{GeV}, \quad |y_{\text{jet}}| < 4.5, \quad p_{T,l} > 20\text{GeV}, \quad |y_l| < 2.5, \\
 \Delta R_{ll} > 0.2, \quad \Delta R_{l\text{jet}} > 0.5, \quad 66\text{GeV} < M_{ll} < 116\text{GeV}.
 \end{aligned}
 \tag{3.8}$$

for the transverse momenta, rapidities, rapidity–azimuthal angle separation, and invariant mass. In addition, the photon energy fraction z_γ in a jet must be below 0.7.

Using the set-up defined above we find for the cross section the results shown in Table 1. The total cross section is dominated by processes with external gluons, which amount to 77%. For our set of cuts, the corresponding relative EW corrections are at the level of -2.5% and similar for all channels.

In Fig. 3 we present results for the differential cross section as a function of the transverse momentum of the harder jet and of the negatively charged lepton. Both distributions decrease over five orders of magnitude in the displayed p_T ranges. While the four-quark channels dominate for high p_{T,j_1} , their contribution stays at the level of 25% for all p_{T,l^-} . The bottom-quark contributions, which are shown separately, are below 5% and become less important for large transverse momenta. The electroweak corrections are negative and reach about -20% for $p_{T,j_1} \approx 1\text{TeV}$ and $p_{T,l^-} \approx 600\text{GeV}$. The large negative corrections result from Sudakov logarithms in the EW loop contributions. The (subtracted) real corrections from photon or gluon emission stay below 2%. We also show the experimental statistical uncertainty corresponding to an integrated luminosity of 20fb^{-1} .

4. Conclusions

We have presented results for the $\mathcal{O}(\alpha_s^2\alpha^3)$ contributions to the production of $l^+l^- + 2$ jets at the LHC. These include electroweak corrections to the LO QCD diagrams and QCD corrections

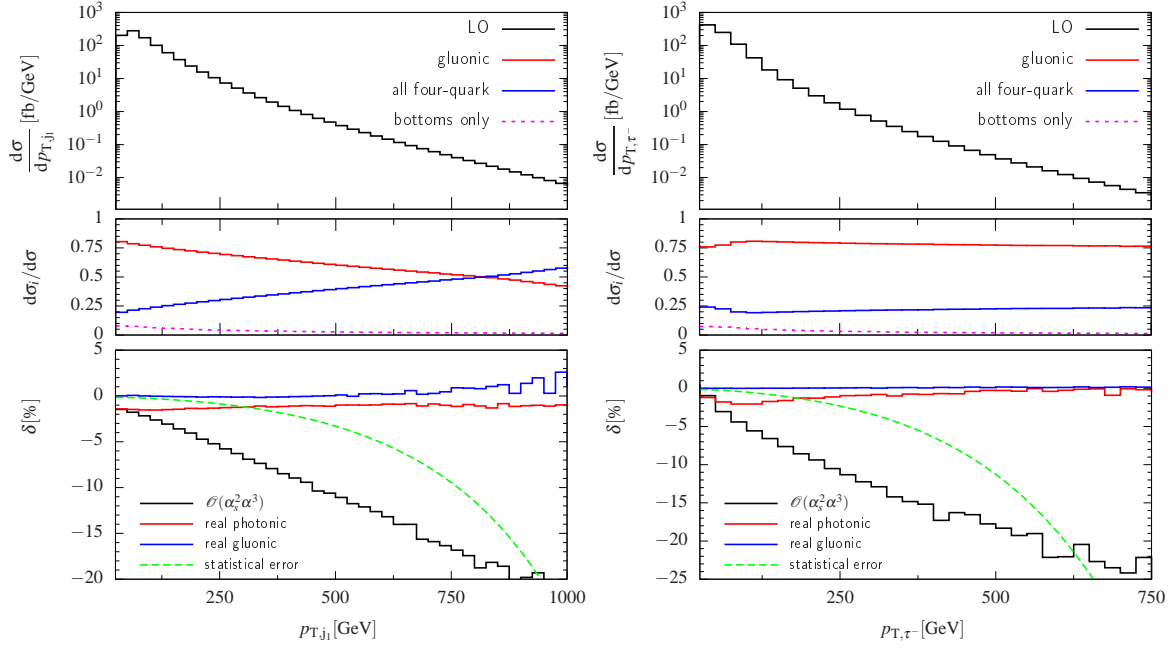


Figure 3: Distributions of the transverse momenta of the harder jet j_1 (left) and the negatively charged lepton l^- (right) at the 8TeV LHC at LO (black). The central panels show the relative contributions of gluonic (red), four-quark (blue) and bottom (magenta, dashed) channels. In the lower panels we show the total relative corrections (black) from $\mathcal{O}(\alpha_s^2 \alpha^3)$ contributions, the included real photonic (red) and real gluonic (blue) corrections together with the statistical error (green, dashed).

to the interferences between LO QCD and EW diagrams. The results have been obtained with the amplitude generator RECOLA and the tensor-integral library COLLIER. The electroweak corrections turn out to be at the level of -2% for inclusive cross sections. In the high-energy tails of distributions large EW corrections appear which can be attributed to EW Sudakov logarithms.

Acknowledgements

This work was supported in part by the Deutsche Forschungsgemeinschaft (DFG) under reference number DE 623/2-1.

References

- [1] C. F. Berger, et al., Phys. Rev. D **78** (2008) 036003 [arXiv:0803.4180 [hep-ph]].
- [2] W. T. Giele and G. Zanderighi, JHEP **0806** (2008) 038 [arXiv:0805.2152 [hep-ph]].
- [3] A. Lazopoulos, arXiv:0812.2998 [hep-ph].
- [4] W. Giele, Z. Kunszt and J. Winter, Nucl. Phys. B **840** (2010) 214 [arXiv:0911.1962 [hep-ph]].
- [5] S. Badger, B. Biedermann and P. Uwer, Comput. Phys. Commun. **182** (2011) 1674 [arXiv:1011.2900 [hep-ph]].
- [6] V. Hirschi, et al., JHEP **1105** (2011) 044 [arXiv:1103.0621 [hep-ph]].
- [7] G. Bevilacqua, et al., arXiv:1110.1499 [hep-ph].

- [8] G. Cullen, et al., *Eur. Phys. J. C* **72** (2012) 1889 [arXiv:1111.2034 [hep-ph]].
- [9] S. Actis, et al., *JHEP* **1304** (2013) 037 [arXiv:1211.6316 [hep-ph]].
- [10] S. Actis, A. Denner, L. Hofer, A. Scharf and S. Uccirati, these proceedings.
- [11] A. van Hameren, *JHEP* **0907** (2009) 088 [arXiv:0905.1005 [hep-ph]].
- [12] J. M. Campbell and R. K. Ellis, *Phys. Rev. D* **65** (2002) 113007 [hep-ph/0202176];
J. M. Campbell, R. K. Ellis and D. L. Rainwater, *Phys. Rev. D* **68** (2003) 094021 [hep-ph/0308195].
- [13] C. Oleari and D. Zeppenfeld, *Phys. Rev. D* **69** (2004) 093004 [hep-ph/0310156].
- [14] M. Chiesa, et al., *Phys. Rev. Lett.* **111** (2013) 121801 [arXiv:1305.6837 [hep-ph]].
- [15] A. Denner and S. Dittmaier, *Nucl. Phys. B* **658** (2003) 175 [hep-ph/0212259].
- [16] A. Denner and S. Dittmaier, *Nucl. Phys. B* **734** (2006) 62 [hep-ph/0509141].
- [17] A. Denner and S. Dittmaier, *Nucl. Phys. B* **844** (2011) 199 [arXiv:1005.2076 [hep-ph]].
- [18] A. Denner, S. Dittmaier and L. Hofer, in preparation.
- [19] F. Cascioli, P. Maierhöfer and S. Pozzorini, *Phys. Rev. Lett.* **108** (2012) 111601 [arXiv:1111.5206 [hep-ph]].
- [20] F. Cascioli, P. Maierhöfer and S. Pozzorini, these proceedings.
- [21] G. Passarino and M. J. G. Veltman, *Nucl. Phys. B* **160** (1979) 151.
- [22] G. 't Hooft and M. J. G. Veltman, *Nucl. Phys. B* **153** (1979) 365.
- [23] A. Denner, S. Dittmaier, M. Roth and D. Wackerroth, *Nucl. Phys. B* **560** (1999) 33 [hep-ph/9904472].
- [24] A. Denner, S. Dittmaier, M. Roth and L. H. Wieders, *Nucl. Phys. B* **724** (2005) 247 [Erratum-ibid. B **854** (2012) 504] [hep-ph/0505042].
- [25] A. Denner and S. Dittmaier, *Nucl. Phys. Proc. Suppl.* **160** (2006) 22 [hep-ph/0605312].
- [26] S. Catani and M. H. Seymour, *Nucl. Phys. B* **485** (1997) 291 [Erratum-ibid. B **510** (1998) 503] [hep-ph/9605323].
- [27] A. Denner, S. Dittmaier, T. Gehrmann and C. Kurz, *Nucl. Phys.* **B836** (2010) 37 [arXiv:1003.0986 [hep-ph]].
- [28] E. W. N. Glover and A. G. Morgan, *Z. Phys. C* **62** (1994) 311;
D. Buskulic *et al.* [ALEPH Collaboration], *Z. Phys. C* **69** (1996) 365.
- [29] T. Motz, PhD thesis, Zürich 2011.
- [30] T. Hahn, *Comput. Phys. Commun.* **140** (2001) 418 [hep-ph/0012260].
- [31] T. Hahn and C. Schappacher, *Comput. Phys. Commun.* **143** (2002) 54 [hep-ph/0105349].
- [32] T. Hahn and M. Pérez-Victoria, *Comput. Phys. Commun.* **118** (1999) 153 [hep-ph/9807565].
- [33] E. Accomando, A. Denner and C. Meier, *Eur. Phys. J. C* **47** (2006) 125 [hep-ph/0509234].
- [34] S. Dittmaier and M. Roth, *Nucl. Phys. B* **642** (2002) 307 [hep-ph/0206070].
- [35] A. D. Martin *et al.*, *Eur. Phys. J. C* **63**, (2009) 189 [arXiv:0901.0002 [hep-ph]].
- [36] M. Cacciari, G. P. Salam and G. Soyez, *JHEP* **0804** (2008) 063 [arXiv:0802.1189 [hep-ph]].